**Solid Freeform Fabrication 2018: Proceedings of the 29th Annual International
Solid Freeform Fabrication Symposium – An Additive Manufacturing Conference**

HYBRID MANUFACTURING WITH FDM TECHNOLOGY FOR ENABLING POWER ELECTRONICS COMPONENT FABRICATION

Jose L. Coronel Jr.*, Kazi Md Masum Billah*, Carlos F. Acosta Carrasco*, Sol A. Barraza*,
Ryan B. Wicker *, and David Espalin*

*Department of Mechanical Engineering
The University of Texas at El Paso, El Paso, TX, 79968
*W.M. Keck Center for 3D Innovation, El Paso, TX, 79968
Corresponding author: jlcoronel@miners.utep.edu

Abstract

The introduction of Kapton coated wires within a printed substrate presents the opportunity to design and fabricate power electronics components. Preventing dielectric breakdown of the printed substrate, the ultrasonic embedding approach enables complex geometrical embedding through customized software. This work presents the effective embedding of large diameter (14 AWG) kapton coated litz wire into polycarbonate (PC) substrate. Custom software allowed for generation of embedding toolpaths directly from the CAD model of the designed coupon. Results showed the most successful embedding paths were circular pre-formed cavities. Through characterization of a myriad of printed samples, an approach was developed for embedding large diameter wire. Through the use of the Foundry Multi^{3D} System, the increased complexity of embedded electronic parts can further impulse the implementation of hybrid additive manufacturing in large scale applications.

1. Introduction

The definition of hybrid manufacturing has been well established as an amalgamation of two or more manufacturing processes to fabricate parts within a simplified process chain, and a condensed amount of time. In conventional manufacturing, work was performed by Jeng *et al.*, (2001) in the development of a hybrid process by combining selective laser cladding (SLC) and three-axis milling. Hybrid processes are not exclusive to multiple machines, as the use of multiple cycles within one machine could achieve "hybridization". Hur *et al.*, (2002) developed a hybrid rapid prototyping process that implemented two cycles of operation. The first cycle involved front and back machining, while the second cycle implemented drilling, milling, and grinding for achieving the final part. Extending beyond conventional means, hybrid additive manufacturing (AM) allows for the fabrication of complex geometries due to collaborative processes. For example, Karunakaran *et al.*, (2010) and Du *et al.*, (2016**)** presented a hybrid system that made use of selective laser melting (SLM), an AM method, with the addition of milling, a subtractive process. Lee *et al.*, (2014**)** developed a hybrid rapid prototyping system by integrating a Fused Deposition Modeling (FDM) nozzle, with a cutting spindle on a five-axis desktop machine.

In polymer material extrusion AM, access to every layer during part fabrication has enabled an increase in component functionality. Multifunctionality refers to the ability of a component to be utilized beyond structural purposes. Espalin *et al.*, (2014**)** described a method of adding electrical functionality by implementing wire embedding on FDM printed thermoplastic substrates. Other work was performed to add electrical and magnetic functionality within plastics by introducing silver based conductive inks and solid copper wire [Shemelya *et al*., (2015)(2013); Joe Lopes *et al.*, (2012)]. Research conducted at the W.M. Keck Center for 3D Innovation, in pursuit of hybrid manufacturing of multifunctional components, led to the development of the Foundry Multi^{3D} System that incorporates ultrasonic wire embedding. Shown in Figure 1, the Foundry Multi^{3D} System consists of two FDM Fortus 400mc (Stratasys, Eden Prairie, MN, USA) industrial printers, a computer numerical control (CNC) router (LC 3024 CNC), and a six-axis robotic arm (Yaskawa Motoman MH50, Miamisburg, OH, USA)(Ambriz et al. 2017). Through modification of the CNC router, additional processes were implemented to include the ability to machine, embed foils and wires, and pick and place electronic components (Coronel *et al.*, 2017). Leveraging the ability to interrupt the printing process, a portable build platform was made to transfer the workpiece to the CNC for embedding, machining, etc., then be returned to the FDM printers. Overall, the Foundry Multi^{3D} System facilitates the fabrication of 3D printed electronics.

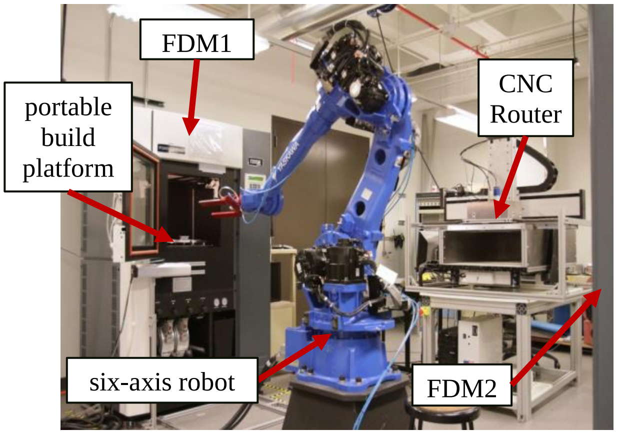

Figure 1: Foundry Multi^{3D} System

Integrating electrical functionality to additively manufactured structures is possible through UTEP's patent-pending wire embedding technology. Ultrasonic consolidation has been utilized in several applications, such as bond formation between aluminum matrix and SiC fiber Yang *et al.*, (2009). Although significant work has been performed in ultrasonic consolidation of metal matrix composites Sriraman *et al.*, (2014), this method has been adopted for the ultrasonic welding of plastic as well Yousefpour *et al.*, (2004). Hybrid AM was accomplished in this study, by adopting a commercially available ultrasonic welding tool on the CNC router of the Foundry Multi^{3D} System. This allowed for the embedding of kapton coated litz wire, traditionally used for power electronics. Kapton coated wire permits the use of high currents, while preventing dielectric breakdown of the substrate. The work presented, describes the approach for embedding large diameter kapton coated wires for future use in power electronics component fabrication, including stators for electric motors.

2. Approach

In general, ideal wire embedding characteristics include minimal part deformation, adhesion between the wire and substrate, and dimensional accuracy. Wire should be flush with the surface, as surface uniformity is essential for continued printing over the embedded substrate. Deformation would be evidenced by heat damage, displaced material, and physical warping of the part. Figure 2 shows a printed polycarbonate (PC) coupon upon which two sizes of kapton coated wires were embedded. The three wires on the right were 28 AWG wires, while the single wire on the left was a 14 AWG wire. The cross section of the coupon was observed with an OGP SmartScope Flash 250 (OGP, Rochester, NY). This initial experiment set the premise for the presented research. When the 28 AWG wire was embedded, PC material was found to be completely surrounding the

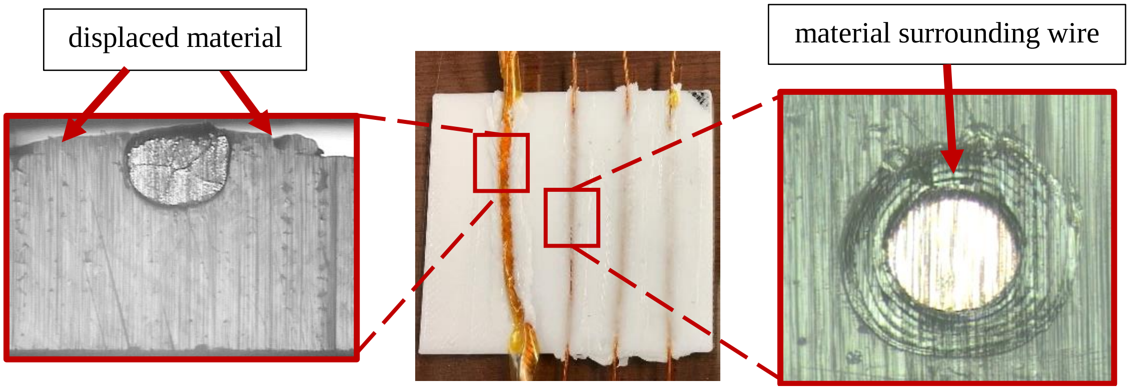

Figure 2: Embedded wires with cross-sectional views

perimeter of the wire. Using previously described criteria, the 28 AWG wires were characterized as well embedded. For the 14 AWG wire, material displacement was observed, in addition to the wire veering from the intended embedding path. An approach was developed through the use of preformed cavities, to allow the proper embedding of large diameter kapton coated wire. Experimental approach and results are discussed, as well as the possible applications for this technology as it pertains to hybrid additive manufacturing and power electronics.

For all experimentation, PC specimen were printed on the Foundry Multi^{3D} System, where once fabricated, the robot arm would transfer them into the CNC for embedding. A commercially available ultrasonic welding tool was used for embedding. The ultrasonic vibrations of the tool heated the printed substrate, causing plastic deformation to allow for the wire to be introduced into the thermoplastic. Figure 3 shows a schematic of the ultrasonic wire embedding tool that was mounted on the CNC router. This tool utilized several horns, depending on the application. Although some horns were designed to simultaneously feed wire and secure it to the plastic, the horn used for these experiments was a flat tip horn that traversed over the manually laid wire. The wide range of embedded wire options required differing approaches to allow for proper embedding. Often, small diameter wires could be fed through a specific horn and embed into a flat substrate without significant struggle. This was attributed to the fact that material displaced by their introduction was minimal. For large diameter wire this was not the case. The material displaced by introducing large diameter wires significantly hindered the ability to evenly deposit material on the surface of the substrate. For this reason, cavities were introduced into the substrate design. The preformed cavities would allow for the wire to be guided, for improved dimensional accuracy, while embedded completely to allow for subsequent material deposition.

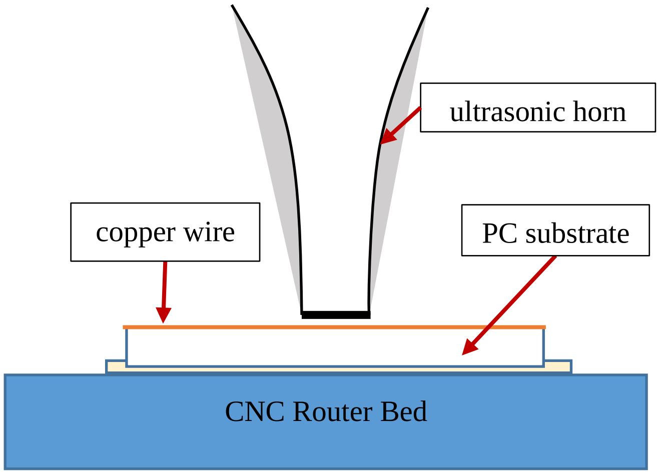

Figure 3: Ultrasonic embedding schematic

Several tests were performed to understand the embedding process, and the effect of generated temperature between the tip and the substrate. Infrared thermography

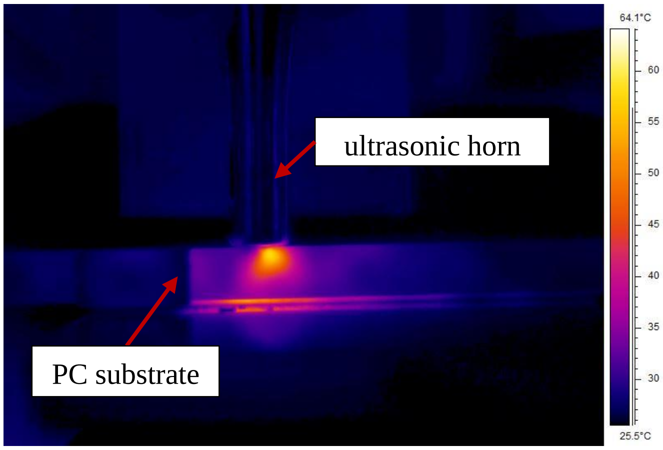

Figure 4: IR thermography of ultrasonic embedding

was used to aid in determining the embedding speed that would circumvent excessive melting and deformation of the plastic. A sample IR thermography result is shown in Figure 4. The figure captures the ultrasonic horn contacting the plastic substrate while ultrasonically embedding a 28 AWG wire. Localized heat generation was observed at the contact point, where the temperature reached an approximate range of 50-55°C. The temperature was relatively low compared to the glass transition temperature of the polycarbonate substrate (~145°C), let alone the melting temperature (~280°C). These results proved that ultrasonic embedding does not rely specifically on heat generation, but rather plastic deformation of material, to allow the wire to be embedded.

3. Experiment

Embedding low gauge wire into a plastic component proved to be a challenge. Material displacement due to large diameter wires, prevents subsequent material extrusion. Therefore, cavities were implemented to introduce wire in a feasible manner, without compromising the fabrication of the component. The cavity geometries were selected based on the simplest shapes that a circular wire could be introduced into. With the flexibility of 3D printing, four different cavity geometries were fabricated; a circle, a square, and two equilateral triangles (regular and inverted), shown in Figure 5. These cavities were designed using Autodesk's Fusion 360 software and manufactured on a Fortus 400mc within the Foundry System. The coupons were all 1x1 inches square, and the 14 AWG kapton coated litz wire was used as the standard for all testing. Litz wire

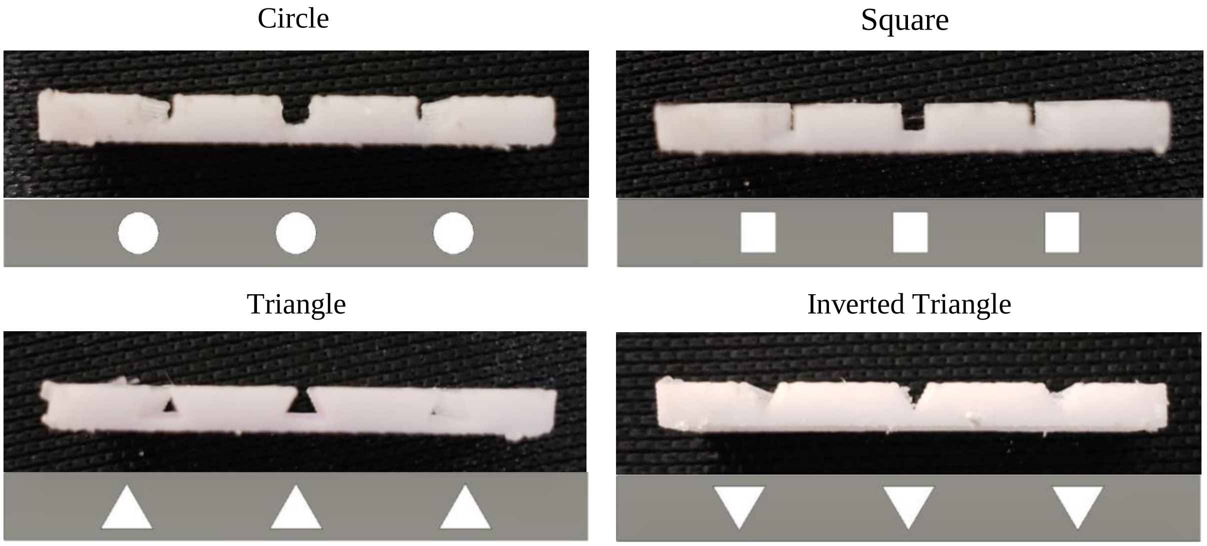

Figure 5. Design and fabrication of preformed cavity

Table 1: Dimensional Accuracy for Printed Specimens

Geometry	Sample Number	Diameter (inch)	Geometry	Sample Number	Base (inch)	Height (inch)
Circle	1	0.073	**Triangle**	1	0.063	0.053
	2	0.068		2	0.061	0.052
	3	0.070		3	0.059	0.048
		Length (inch)			**Base (inch)**	**Height (inch)**
Square	1	0.058	**Inverted triangle**	1	0.091	0.083
	2	0.057		2	0.094	0.087
	3	0.057		3	0.092	0.089

is composed of multiple wire strands, which made the diameter and area vary. The average diameter for the 14 AWG wire was 0.066 inches. Utilizing the cross-sectional area of the wire, the areas for the cavities were determined. The circular cavity was made 0.07 inches so that there would be enough space for the wire to be introduced. Based on the area of the circular cavity, the other cavities were designed. Another factor in cavity size, was the manufacturing capabilities of the printer. Layer thickness was set to 0.01 inches, which resulted in some cavities being slightly larger because the size was rounded up. Table 1 shows the dimensions of the three cavities that were printed per sample. Each sample was inspected with the OGP SmartScope, from which the dimensions were recorded.

The experimentation involved using the flat ultrasonic horn on the Foundry System. Pauses were strategically placed such that the entirety of each geometrical cavity was formed. The specimen with the open cavities were transferred from the Fortus 400mc via robot arm, into the CNC router with the ultrasonic horn assembly. The wires were manually laid over their respective cavity, and the horn traversed over each wire. Embedding the wire into the thermoplastic required more than just the ultrasonic tool. The CNC gantry system was prepared with a complimentary software add-in. To obtain accurate lines throughout the embedding

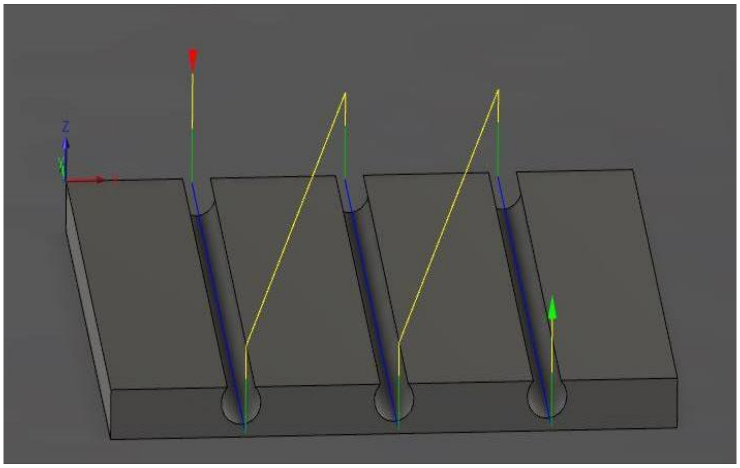

Figure 6: Cavity embedding and results

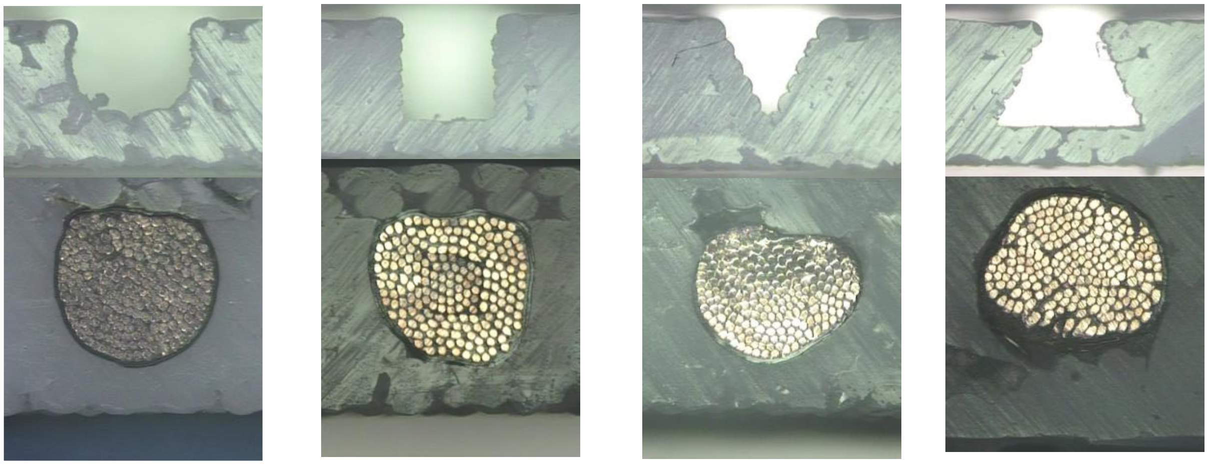

Figure 7: Cross sectional results

process, Fusion 360 was utilized to serve as a modeler. In Figure 6, the wire paths were added to the CAD and by using Fusion's CAM package, the paths were processed. A custom post process plug-in was added to Fusion's CAM to obtain a GCODE. This GCODE file was then used on the CNC router for wire embedding implementation. The file includes parameters to turn on/off the ultrasonic tool, jog speed, and pauses for each circuitry.

After testing, it was determined that a 60 mm/min jog speed for the traversing ultrasonic tool provided the best embedding. Figure 7 shows the cross section of each geometry at both the un-embedded and embedded state. As the figure shows, the circular cavity resulted in the wire with the least amount of deformation. The clear boundary line in the circular sample suggests a high level of wire-plastic contact throughout the circumference. This wire-plastic interface was not as pronounced in the other samples. The square cavity showed significant wire deformation, as well as gaps in the top two layers of the sample. The inverted triangle sample had acceptable wire-plastic contact and showed no significant part deformation, however pronounced porosity was seen in the top two layers of printing. The upright triangle sample underwent significant deformation as it was embedded. Due to the base of the triangular cavity being larger than the wire diameter, some porosity was found on the underside of the wire. This experimentation led to the conclussion that a circular cavity would result in better embedding. Figure 8 shows tests that were replicated for only circular cavities. Using the optimal speed of 60 mm/min, three samples with

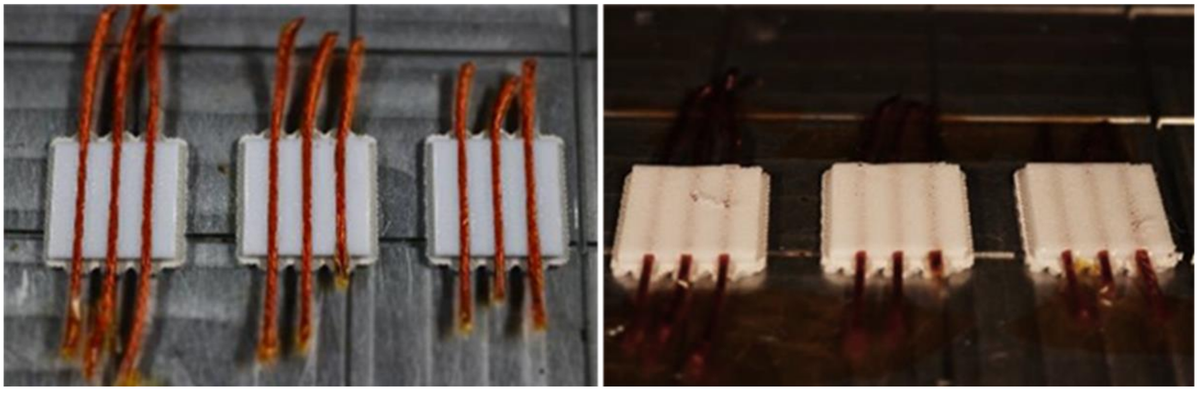

Figure 8: Embedding of kapton coated litz wire in circular cavities

three circular cavities were printed. Resulting specimen showed that there were minimal surface defects when printing was resumed over the embedded wires. From previous experience, it is expected that the small defects would be removed once additional material extrudes over the surface.

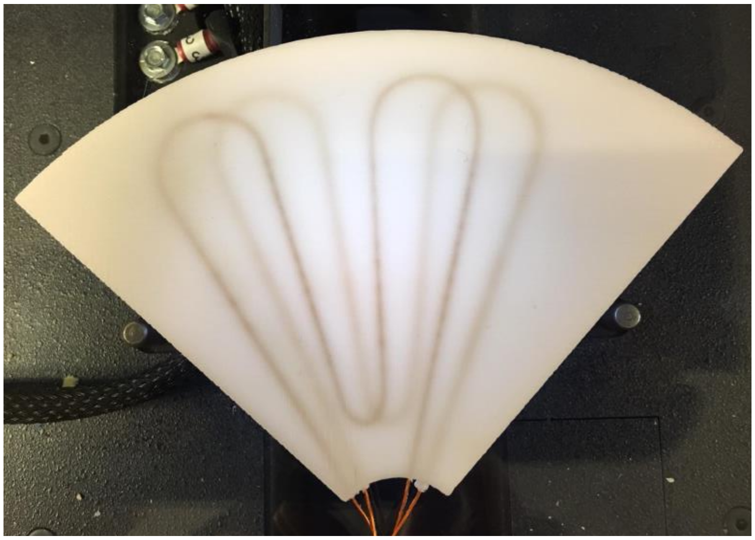

Figure 9: Quarter stator for an axial flux motor

4. Conclusion

The demonstration of ultrasonic wire embedding on thermoplastic substrate indicates that it is possible to fabricate 3D electronics with embedded circuitry or wire routing. Large diameter wire embedding will facilitate the fabrication process of power electronics, such as electric motor components. The presented work showed that circular cavity designs can be implemented to embed the gauge of wire necessary for power electronics. The cavities not only facilitated the placement of the wire, but helped stake the wire to the substrate without significant deformation. An attempt was taken to fabricate a quarter stator of an axial flux motor, shown in **Error! Reference source not found.**. In this case, 28 AWG kapton coated litz wire was embedded within PC substrate to mimic the winding of a stator. Benefits of AM for this specific application compared to traditional methods, would be the cost reduction of tooling, shortening the fabrication process chain, and automation of wire winding. Although, the operational temperature and material breakdown strength are the key design criteria for an axial motor/generator, this multi process AM method can be employed after selecting the thermoplastic material that will satisfy the operational requirements. Moreover, it is expected that work with hybrid AM involving wire embedding, could lead to fabrication of power electronic components in the future.

5. References

Ambriz, S., Coronel, J., Zinniel, B., Schloesser, R., Kim, C., Perez, M., ... & Wicker, R. B. (2017). Material handling and registration for an additive manufacturing-based hybrid system. *Journal of Manufacturing Systems*, *45*, 17-27.

Coronel, J. L., Fehr, K. H., Kelly, D. D., Espalin, D., & Wicker, R. B. (2017, May). Increasing component functionality via multi-process additive manufacturing. In *Micro-and Nanotechnology Sensors, Systems, and Applications IX* (Vol. 10194, p. 101941F). International Society for Optics and Photonics.

Dehoff, R. R., & Babu, S. S. (2010). Characterization of interfacial microstructures in 3003 aluminum alloy blocks fabricated by ultrasonic additive manufacturing. *Acta Materialia*, *58*(13), 4305-4315.

Du, W., Bai, Q., & Zhang, B. (2016). A novel method for additive/subtractive hybrid manufacturing of metallic parts. *Procedia Manufacturing*, *5*, 1018-1030.

Espalin, D., Muse, D. W., MacDonald, E., & Wicker, R. B. (2014). 3D Printing multifunctionality: structures with electronics. *The International Journal of Advanced Manufacturing Technology*, *72*(5-8), 963-978.

Hur, J., Lee, K., & Kim, J. (2002). Hybrid rapid prototyping system using machining and deposition. *Computer-Aided Design*, *34*(10), 741-754.

Jeng, Jeng Ywan, and Ming Ching Lin. 2001. "Mold Fabrication and Modification Using Hybrid Processes of Selective Laser Cladding and Milling." *Journal of Materials Processing Technology* 110 (1): 98–103.

Joe Lopes, A., MacDonald, E., & Wicker, R. B. (2012). Integrating stereolithography and direct print technologies for 3D structural electronics fabrication. *Rapid Prototyping Journal*, *18*(2), 129-143.

Karunakaran, K. P., Suryakumar, S., Pushpa, V., & Akula, S. (2010). Low cost integration of additive and subtractive processes for hybrid layered manufacturing. *Robotics and Computer-Integrated Manufacturing*, *26*(5), 490-499.

Kelly, G. S., Just Jr, M. S., Advani, S. G., & Gillespie Jr, J. W. (2014). Energy and bond strength development during ultrasonic consolidation. *Journal of materials processing technology*, *214*(8), 1665-1672.

Lee, W. C., Wei, C. C., & Chung, S. C. (2014). Development of a hybrid rapid prototyping system using low-cost fused deposition modeling and five-axis machining. *Journal of Materials Processing Technology*, *214*(11), 2366-2374.

Shemelya, C., Cedillos, F., Aguilera, E., Maestas, E., Ramos, J., Espalin, D., ... & MacDonald, E. (2013, November). 3D printed capacitive sensors. In *SENSORS, 2013 IEEE* (pp. 1-4). IEEE.

Shemelya, C., Cedillos, F., Aguilera, E., Espalin, D., Muse, D., Wicker, R., & MacDonald, E. (2015). Encapsulated copper wire and copper mesh capacitive sensing for 3-D printing applications. *IEEE Sensors Journal*, *15*(2), 1280-1286.

Sriraman, M. R., Babu, S. S., & Short, M. (2010). Bonding characteristics during very high power ultrasonic additive manufacturing of copper. *Scripta Materialia*, *62*(8), 560-563.

Yang, Y., Ram, G. J., & Stucker, B. E. (2009). Bond formation and fiber embedment during ultrasonic consolidation. *Journal of Materials Processing Technology*, *209*(10), 4915-4924.

Yousefpour, A., Hojjati, M., & Immarigeon, J. P. (2004). Fusion bonding/welding of thermoplastic composites. *Journal of Thermoplastic composite materials*, *17*(4), 303-341.